

EFFECT OF NANO-PAPER COATING ON FLEXURAL PROPERTIES OF A FIRE-TREATED GLASS FIBER-REINFORCED POLYESTER COMPOSITE

Jamie Skovron, Jinfeng Zhuge, Ali P. Gordon, Jayanta Kapat, and Jihua Gou

Department of Mechanical, Materials, and Aerospace Engineering
University of Central Florida, Orlando, FL USA

Keywords: Flexure testing, rupture, reinforced composite, thermo mechanical

Abstract

Planned re-usable aerospace vehicles require materials with high specific strength to withstand thermal shock associated with repeated re-entry into Earth's atmosphere. Composites, such as glass fiber-reinforced polyester (GRP), have rapidly become preferred for high value structural components requiring high specific strength and durability. Their ability to sustain high tensile loads, impact loads, and the like, has allowed them to be used as light-transmitting panels, fuselages, nose cones, and combustor nozzles. As a part of service conditions, heat flux strongly alters mechanical properties with exposure time. The effect of including a carbon nano-paper coating on the monotonic flexural properties of a GRP composite is analyzed. The nano-paper acts as a thermal barrier to protect the underlying material in the presence of above glass-transition temperatures. A series of three-point bend experiments was performed on specimen-sized samples of composites subjected to various levels of heat fluxes across numerous exposure times. Analysis of these experiments reveals trends in the deformation mechanisms of these materials near failure. Correlations of flexural modulus and critical load are used to develop models for strength.

1. Introduction

The use of composites has grown rapidly due to their attractive mechanical properties in comparison to existing conventional materials. Aircraft manufacturers have incorporated composites into more recent designs as a consequence. Frames of first-generation airplanes were constructed from wood, steel wire, and silk until it progressed to aluminum. This material has historically been the primary choice due to its low density, yet high tensile strength; however, more recently, the need for higher fuel economy has continued to alter aerospace materials selection [1]. The popularity of composites has grown tremendously in current commercial aircrafts. Components of new generation commercial aircrafts have grown from 12% to 50% by weight for composites; while aluminum has decreased from 50% to 20% by weight [2]. Advanced research has demonstrated through testing, that composites have high specific strength at ambient temperatures (below 212°F) and thus have grown in reputation. This design philosophy is also applicable through development activities of re-usable launch vehicles. Such spacecrafts must be able to withstand the cold, near absolute zero, temperature occurring outside of the limits of Earth's atmosphere, but also endure the high temperature of approximately 1260°C (2300°F) during re-entry [3]. The spacecraft components should be designed to endure these repetitive thermal exposures for several mission cycles while simultaneously being mechanically loaded. Re-entry vehicles that have traveled from Earth to Mars have encountered temperatures that exceed 1500°C (2732°F) [4]. It is essential that the selected fuselage materials

be able to withstand these high temperatures without compromising structural integrity. With composites having such a high strength to density ratio, a range of 0.05 to 1 MJ/kg , they must be among the top competitors for material selection [1]. Design engineers must understand how composites will perform under certain loading and thermal conditions.

The focus of this study is to characterize how thermal barrier carbon nano-paper affects the flexural properties of GRP composites. Nano-paper coatings are applied to a GRP composite, which is then exposed to an applied heat flux and various exposure times. The heat flux is used to simulate the high re-entry temperatures. Following the return to room temperature (72°F), flexural experiments are performed on the coated and uncoated samples. Results of the three-point bend test are outputted in the form of a force-displacement curve. The mechanical properties related to elastic, plastic, and rupture behavior of the samples are subsequently derived. Based on the experimental results and microscopy, analytical models are developed to predict the mechanical response of carbon nano-paper coated GRP composites under service conditions.

The candidate material for the current study is detailed in Sec. 2, and the experimental mechanics approach is described in Sec. 3. Section 4 of the current work focuses on the elastic properties of the GRP composite materials, while Sec. 5 covers observations on the rupture trends, respectively, that were developed. Conclusions and avenues for continued research are outlined in Sec. 6.

2. Glass-Fiber Reinforced Polyester (GRP) Composites

Glass-fiber reinforced polyester (GRP) composites, Fig. 1, are composed of multiple layers adhered by an orthophthalic resin. The polyester substrate material is reinforced with glass fibers whose specific strength is approximately 0.94 MJ/kg , this value gives the composite its high specific strength [5]. Use of GRP composites in more widespread applications is limited by their poor fire resistivity [6]; designers seek a thermal barrier to protect the effectiveness of the material. Carbon nano-paper is selected as the protective barrier that acts not only as a thermal barrier, but absorbs the heat that would otherwise penetrate the composite and compromise the structural integrity [7]. This study is focused on whether the carbon nano-paper can considerably protect the flexural properties of the material in the presence of high temperatures. Figure 2 details the dimensions of the uncoated and coated GRP composites.

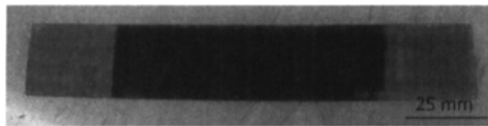


Figure 1: GRP composite with flux induced side face up.

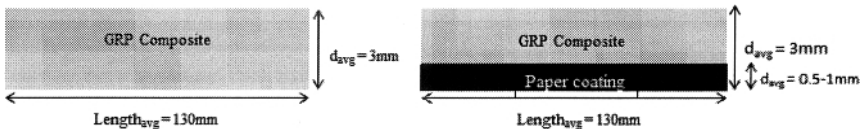


Figure 2: Dimensions of uncoated and coated GRP samples.

3. Experimental Approach

The GRP composites were exposed to a predetermined flux level and exposure time as outlined in Table 1.

Table 1: Heat treatment for the post fire 3 point bending test.

Applied Heat Flux (kW/m^2)	Exposure Time (s)
25	0, 120, 180, 240, 300
35	0, 60, 100, 140, 180
50	0, 40, 80, 120, 150
75	0, 20, 50, 75, 100
100	0, 15, 40, 70, 100

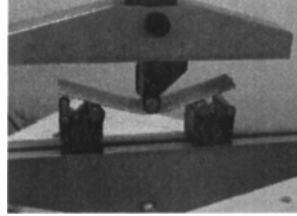


Figure 3: Three-point bend test experimental setup

Mechanical experiments were then performed on samples of the candidate material to determine the mechanical effect of firing on the residual mechanical properties. Flexure experiments are preferred on composite samples since the imparted mechanical load bears resemblance to service conditions of the full scale components of these materials. Flexure tests were administered in accordance with the ASTM D790-10 standard [8]. A total of 117 samples underwent three-point bending, Figure 3, using an Instron 3369 with a load capacity of $50kN$. The fire-treated side of the sample was placed face down during the three-point bending test. The support span, L , was $76mm$ and the crosshead motion rate, denoted by $\dot{\delta}$ was $2.4 mm/min$. The experiment would cease if either the centerline deflection of the specimen reached $12mm$ or there was a dramatic drop in the load-deflection curve. The mechanical properties of these specimens such as modulus of elasticity in bending and rupture force can be calculated from the outputted raw data. By inputting variables into the model, the elastic modulus in bending (E_B) was able to be calculated.

$$E_B = \frac{L^3 m}{4bd^3} \quad (1)$$

Here, L is the support span (mm) between the two supporting rollers, m is the slope of the tangent to the initial straight-line portion of the load-deflection curve (kN/mm), b is the width of the beam tested (mm), and d is the thickness of the beam tested (mm).

4. Elastic Modulus

The elastic modulus in bending of the GRP composites was determined after the three-point bend test by utilizing Eq. 1. By inputting the parameters and data from the experimental procedure, the elastic modulus for each sample was calculated. The values for each flux-time sample set were averaged and used to formulate a model that predicts the elastic modulus based on a designated flux level and exposure time. Post-fire mechanical testing can hinder the true mechanical properties of the GRP composites during service. This deception is present due to the nature of composites as they tend to regain some of their strength after being cooled back down to room temperature [9]. For that reason, a temperature-time dependent model would be problematic to develop. Therefore, the following theorized model depicts the elastic modulus as a function of flux level and exposure time. Past researchers have developed mechanical property

models based on separating the composite into two or three layers, but the drawback to these models is the classification of the different layers. [6,10]. The model presented in this study models the mechanical properties of the uncoated and coated GRP composites based on the flux level and exposure time. The model is to be utilized as a guide-line for the experimental data, any parameters outside the data set cannot be guaranteed for accuracy.

$$E_{Sim} = \sum_{i=0}^2 \sum_{j=0}^2 E_{ij} \phi^i t_{exp}^j \quad (2)$$

In this equation, the flux level, ϕ , has units of kW/m^2 and the exposure time, t_{exp} , has units of seconds. The same model is used to estimate the elastic modulus for the uncoated and coated samples; however, the constants vary. The constants that must be inputted for either the uncoated or coated model are shown in Table II.

Table II: Constants for the elastic modulus model.

Constant	Units	Uncoated Value	Coated Value
E_{00}	GPa	23.28	20.06
E_{21}	s mN	5.802×10^{-5}	4.210×10^{-5}
E_{01}	GPa/s	1.250×10^{-1}	8.219×10^{-2}
E_{11}	$1/\mu m$	-8.545×10^{-3}	-5.626×10^{-3}
E_{10}	$s/\mu m$	-8.364×10^{-2}	-1.166×10^{-1}
E_{02}	$10^6 Mg/ms^4$	0	0
E_{12}	$1 \mu ms$	0	0
E_{20}	$s^4/m^3 g$	0	0
E_{22}	$s^2/m^3 g$	0	0

It was calculated that 93.75% of the uncoated data points fit within +/- 5.GPa of the simulated values. The single data point that was not within this bound was the uncoated sample exposed to a flux level of $25 kW/m^2$ for 120 s. The value obtained experimentally was 21.63GPa, but the simulated value was 14.90GPa.

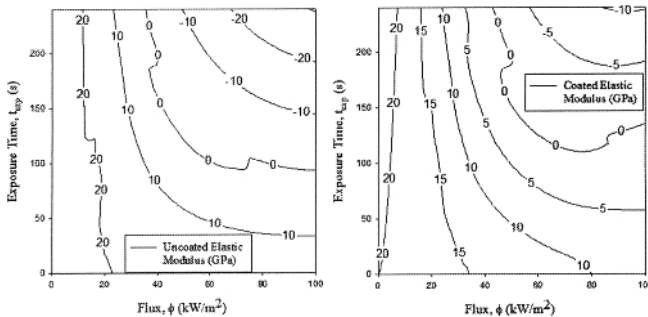


Figure 4: Elastic modulus model for (a) uncoated and (b) coated GRP composites.

It was determined that all of the paper-coated data points fit within +/- 5.GPa of the simulated values. In fact, there are only two data points whose difference between the simulated

and experimental values is greater than $4GPa$. These data points correspond to a heat flux of $25 kW/m^2$ and exposure times of 120 and 180 s. The R-squared value for the uncoated model is 87.7% and 80.8% for the coated one.

According to the data, regardless of ϕ or constant t_{exp} , the elastic modulus decreases for either of these situations. The highest elastic moduli obtained during the experiment were the control samples for the uncoated and coated GRP composites. The control uncoated sample had an average value of $23.28GPa$, while the control paper-coated sample had a mean value of $19.52GPa$. At the opposing end, the samples with the lowest elastic modulus values resulted from the greatest values of ϕ and t_{exp} . The lowest elastic modulus obtained during the uncoated experiments belonged to the sample that had been exposed to a flux of $50 kW/m^2$ for a high exposure time of 120 s. The value was calculated to be as low as $0.895GPa$, which is only 3.84% of the original elastic modulus obtained from the control sample. The coated sample that was exposed to a flux level of $100 kW/m^2$ for 100 s obtained the lowest calculated elastic modulus. This particular sample had a value of $0.778GPa$, a value that is 3.99% of the elastic modulus from the paper-coated control sample.

5. Rupture

The effects of the addition of carbon nano-paper on the normalized maximum force and rupture behavior of the GRP samples are detailed based on the mechanical test data and the microscopy specimen pictures. Due to their nature, composites become pliable when exposed to a high temperature, thus the flexural properties measured after the heat flux process may not give accurate properties of how these composites act during fire [11]. The characterization behavior of composites is a daunting task due to their anisotropic construction. This structural property alters their heat transfer process as when they burn, they release heat, particle-filled vapors, etc., which is followed by charring and finally delamination [11]. From the force-displacement curve, the maximum force applied during the three-point bend test was tabulated for each specimen sample. Three tests were administered for each combination of flux level and exposure time as shown in Table I.

A model was derived that predicts the normalized maximum force for the uncoated and coated samples using the input parameters of flux level and exposure time. The model is only valid for the data obtained during the three-point bend experiments; any values outside the data cannot be confirmed to be accurate. After inspecting the model, any normalized values that are less than 4% of the control specimen return a value that is less than 0. These samples are considered failed due to their low residual values. The constants, F_{ij} , are defined in Table III.

$$F_{Max,Sim} = \sum_{i=0}^2 \sum_{j=0}^2 F_{ij} \phi^i t_{exp}^j \quad (3)$$

The data for each flux level and exposure time combination were averaged and the trends were analyzed. In general it can be concluded that for each flux level set, the longer the exposure time, the lower the maximum force. This is due to the loss of the original material properties, and the material becoming 'charred' and rendered unusable in service conditions.

Table III: Constants for normalized maximum force model

Constant	Units	Uncoated Value	Coated Value
F_{00}	1	1.115	0.9983
F_{10}	m^2/kW	5.779×10^{-3}	2.793×10^{-4}
F_{01}	$l\ s$	1.278×10^{-2}	6.352×10^{-3}
F_{22}	$m^2\ (kN)^2$	4.575×10^{-8}	2.190×10^{-8}
F_{12}	$s\ (Mg)$	-1.861×10^{-6}	-1.030×10^{-6}
F_{11}	$m\ kN$	-5.441×10^{-4}	-2.793×10^{-4}
F_{02}	$1/s^2$	0	0
F_{20}	m^4/MW^2	0	0
F_{21}	m^2s/MN^2	0	0

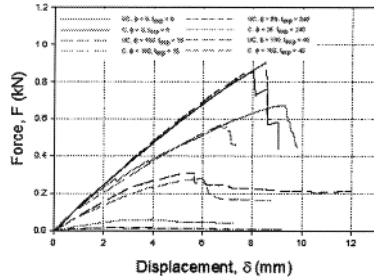


Figure 5: Force-displacement for various data sets

The maximum forces for the uncoated and coated samples were normalized for each flux level. These normalized distributions are shown in Figure 6. One can see in Figure 6(a) that during a heat flux of $25\ kW/m^2$, the maximum force for the paper coated samples exposed to the flux for 180 s have almost three times the original maximum force compared to that of the uncoated samples, normalized values of 0.9598 and 0.3646 respectively. When the samples were exposed to a longer exposure time of 240 s, the normalized values became closer but the paper samples still maintained a higher percent of their original values, 0.222 compared to 0.029. The R-squared value for both the uncoated and coated model is 93.3%.

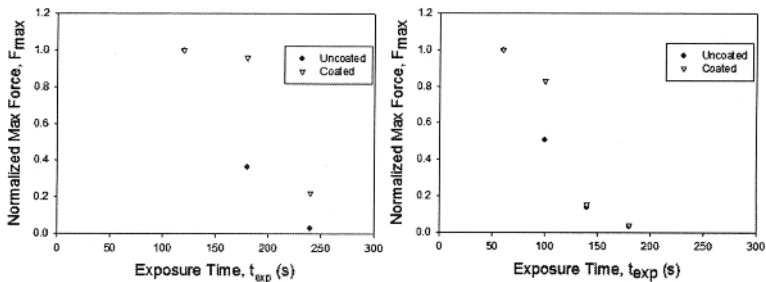


Figure 6: Effects of exposure time on the normalized maximum force for (a) $25\ kW/m^2$ and (b) $35\ kW/m^2$.

The physical appearance of the GRP composites after being subjected to a level of heat flux and a three-point bend test is observed in this section. Figure 7(a) shows the composites exposed to a heat flux of $100\ kW/m^2$ with an exposure time of 70 s. The uncoated sample has continued to fray, in addition to the expansion of the fibers. This expansion is likely due to the gases escaping during the applied heat flux process [11]. The paper on the coated sample has become severely charred and has allowed a greater level of heat flux to penetrate the composite. The penetration of the coated sample is evident due to the increase thickness of the fibers. Fire barrier treatments, such as the carbon nano-paper used in this study, occupy the role of either reflecting the heat back towards the source or delaying the heat penetration towards the underlying composite [11].

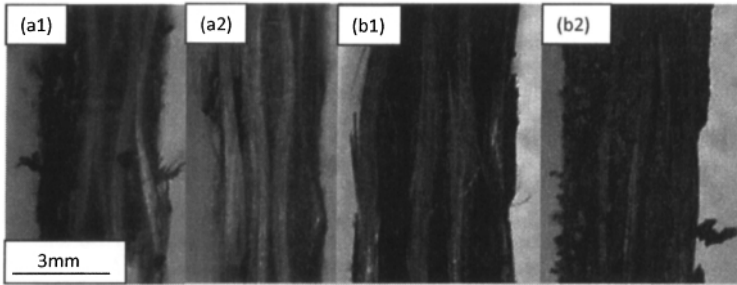


Figure 7: GRP composite in cross-section after being exposed to a heat flux of 100 kW m^{-2} for 70 s then a three-point bend test for (a1) uncoated and (a2) paper coated samples and a heat flux of 100 kW m^{-2} for 100 s for (b1) uncoated and (b2) paper coated samples. The left surface was exposed to the heat source.

Figure 7(b) is at the extreme end of the flux-time combination. The samples shown in Figures 7(b1) and (b2) have been exposed to a level of 100 kW/m^2 for 100 s. Despite both samples having noticeably different physical appearances compared to their associated controls, the coated sample is still in one piece. Figure 7(b1), displays delamination of the composite.

Delamination is considered to be the sign of critical failure of a composite; it is characterized by fraying or ply separation due to interlaminar stresses [12]. This particular sample is to be considered beyond 'failed' due to it experiencing delamination and it being classified as a failed specimen before the three-point bend test. The coated sample was able to endure a three-point bend test, except it only retained a normalized maximum force value of 0.033, equating to 3.3% of the 15 s sample.

6. Conclusion

Glass fiber-reinforced polyester composites used for reusable launch vehicles can experience large declines in their mechanical properties after being exposed to a high heat source. The properties decrease as both the flux level and exposure time increases. The study confirms that the carbon nano-paper helps slow down the degradation process by acting as a thermal barrier between the heat source and the underlying composite. The data suggests that at high exposure times, the paper-coated samples were able to maintain a higher percent of the original elastic modulus compared to that of the uncoated samples. Models to simulate the elastic modulus and normalized maximum force were developed as a guide to understand the properties of GRP composites at various heat flux levels and exposure times.

Future work should be focused towards analyzing the coated and uncoated GRP composites under more extreme temperature values. The temperatures in space ranges from absolute zero to near 2500°F , thus a constitutive mechanical model must be developed for this wide temperature range. One must understand the characterization of these materials at extreme temperatures to ensure proper service.

7. Acknowledgements

The materials presented here are based upon work supported by Office of Naval Research under Grant No. N00014-09-1-0429 and Federal Aviation Administration Center of Excellence for Commercial Space Transportation (FAA COE-CST-AST) under grant number 10CCSTUCF002.

8. References

- [1] Ashby, M. F., 2011. *Materials Selection in Mechanical Design*. 4th ed. Burlington, MA: Butterworth-Heinemann. pp. 12, Chap. 1.
- [2] Hale, J. "Boeing 787 from the Ground Up." *Aero Magazine*. Vol. 4, pp. 17-24, 2006.
- [3] Kulhman, E., "Investigation of high temperature antenna designs for space shuttle," *Antennas and Propagation Society International Symposium*. Vol.12, pp. 210- 213, 1974.
- [4] Rawal, S., "Metal-matrix composites for space applications." *JOM Journal of the Minerals, Metals and Materials Society*. Vol. 53, Issue 4, pp. 14-17, 2001.
- [5] Wambua, P., Ivens, J., Verpoest, I., "Natural fibres: can they replace glass in fibre reinforced plastics?" *Composites Science and Technology*. Vol. 63, Issue 9, pp. 1259-1264, 2003.
- [6] Mouritz, A.P., Mathys, Z., "Post-fire mechanical properties of glass-reinforced polyester composites." *Composites Science and Technology*. Vol. 6, pp. 475-490, 2001.
- [7] Zhuge, J., "Finite Element of Thermo-Mechanical Response of Fiber Reinforced Polymer Composites under Constant Heat Flux." MS. University of Central Florida, Orlando, FL, 2011
- [8] ASTM Standard D790, "Standard Test Methods for Flexural Properties of Unreinforced and Reinforced Plastics and Electrical Insulating Materials," *ASTM International*, West Conshohocken, PA, 2010.
- [9] Kandare, E., Kandola, B.K., Myler, P., Horrocks, A.R., Edwards, G., "Thermo-mechanical responses of fibre-reinforced epoxy composites exposed to high temperature environment: I." *Journal of Composite Structures*. Vol. 26, pp. 3093-3114, 2010.
- [10] Bai, Y., Keller, T., Vallee, T., "Modeling of stiffness of FRP composites under elevated and high temperatures." *Composites Science and Technology*. Vol. 68, pp. 3099-3106, 2008.
- [11] Sorathia, U., Beck, C., Dapp, T., "Residual Strength of Composites during and after Fire Exposure." *Journal of Fire Sciences*. Vol. 11, Issue 3, pp. 255-70, 1993.
- [12] Mallick, P. K., 2008. *Fiber-reinforced Composites: Materials, Manufacturing, and Design*, 3rd Ed, CRC Press, Boca Raton, FL. pp. 474, Chap. 6.